

Dielectric constant of GaAs during a subpicosecond laser-induced phase transition

Y. Siegal, E. N. Glezer, and E. Mazur

Department of Physics and Division of Applied Sciences, Harvard University, Cambridge, Massachusetts 02138

(Received 10 February 1994)

We measured the time evolution of the real and imaginary parts of the dielectric constant of GaAs following femtosecond laser pulse excitation. The data show a collapse of the average optical gap, or average bonding-antibonding energy-level separation. The rate of collapse increases with pump fluence. The decrease in the gap indicates that the pump beam induces a structural transformation from a covalent, tetrahedrally coordinated crystal to a phase with metallic cohesive properties.

Since the suggestion that an electron-hole plasma may play an important role in pulsed laser annealing of semiconductors,¹ a number of calculations have shown that the excitation of a critical density of electron-hole pairs results in structural instability of the lattice.^{2,3} If enough electrons are excited from bonding valence-band states to antibonding conduction-band states, covalent bonding will no longer be able to support the tetrahedrally coordinated crystal structure.⁴ The resulting structural change should manifest itself optically through a decrease of the average optical gap, i.e., the average over k space of direct interband transitions between bonding and antibonding energy levels.^{4,5} A transition to a (semi)metallic state will occur when the average bonding-antibonding splitting is small enough that the conduction-band minimum falls below the valence-band maximum.

Critical electron-hole plasma densities for lattice instability can be created by femtosecond laser pulse excitation because the excited carrier system cannot transfer energy to the lattice on such a short time scale.⁶⁻⁸ Recent experiments using second-harmonic generation and reflectivity probes of semiconductors following excitation with femtosecond laser pulses suggested that a transformation from semiconductor to metal occurs on a subpicosecond time scale.⁹⁻¹¹ However, the interpretation of the second-harmonic results was based on the assumption that changes in the linear dielectric constant play only a minor role in the observed changes in the second-harmonic signal. Unfortunately, the information provided by the reflectivity data in Refs. 9-11 was insufficient to extract the actual response of the dielectric constant to the excitation, leaving the above-mentioned assumption untested. In fact, the data presented in this report show that the changes induced in the linear dielectric constant are unexpectedly large and, contrary to the assumption in previous work, cannot be ignored in analyzing second-harmonic-generation results. Moreover, the dielectric constant is an intrinsic material property of particular importance for theoretical work and, in particular, gives the value of the average optical gap. Unique determination of both the real and imaginary parts of the dielectric constant during this phase transition is thus essential for gaining physical insight into the nature of the transition.

Knowledge of the reflectivity for a particular polarization at two different angles of incidence completely deter-

mines the real and imaginary parts of the dielectric constant for a particular frequency. Optimal sensitivity to changes in the dielectric constant is obtained with angles of incidence near the Brewster angle and polarization for both beams in the plane of incidence.¹² Using two simultaneous 75-fs probe beams, we measured the response of the dielectric constant to laser pulse excitation with subpicosecond time resolution.

Both the pump and the probe beams are derived from a broadband continuum ranging from 550 to 750 nm generated by the output of an amplified colliding pulse mode-locked laser.¹³ The pump beam is amplified in a three-stage amplifier using the dye DCM as the gain medium to select a 20-nm-wide spectral region centered at 635 nm (2.0 eV); the probe-beam amplifier has two stages with a Rhodamine 6G dye selecting a 10-nm-wide spectral region centered at 570 nm (2.2 eV). Both the pump and the probe amplifiers are pumped with the frequency-doubled output of a 10-Hz Nd:YAG (yttrium aluminum garnet) laser. Separate grating pairs compress the pump and the probe pulses to about 75 fs each. The experimental sample is an insulating (110) GaAs wafer (Cr doped, $\rho > 7 \times 10^7 \Omega \text{ cm}$) in air.

To measure the reflectivity at two angles, the probe is split into two beams, which are incident on the sample at 75.8° and at 70.9° from the surface normal, the former corresponding to the Brewster angle for GaAs. Both beams are polarized in the plane of incidence. To reduce temporal and spatial complications in pump-probe overlap due to geometrical effects, the pump beam is incident at 63°, which is as close as practically possible to the probe beams. The polarization of the pump beam is also in the plane of incidence to minimize the pump energy lost to reflection. To monitor a uniformly pumped region, the probe beams are focused to an area about 16 times smaller than the 0.01-mm² focal area of the pump beam on the sample; the probe-beam penetration depth, which depending upon the excitation is never more than 170 nm, is also well within the 270-nm pump-beam penetration depth. The fluence of the pump beam is varied from 0 to 3.2 kJ/m²; that of the probe beams is kept below 0.1 kJ/m² so as not to produce any detectable changes in the dielectric constant to within our experimental resolution. The sample is translated during data collection so that each data point is obtained at a

different spot on the sample.

In converting the reflectivity data to a dielectric constant, we took into account the presence of an oxide layer on the surface of the sample. To this end we measured, without the pump beam, the p -polarized reflectivity of the GaAs sample for angles of incidence ranging from 65° to 80° . Using a three-phase model of air-oxide-GaAs and assuming an index of refraction $n=2$ for the oxide layer,¹⁴ we inferred from the angle dependence of the reflectivity an oxide layer thickness of 4.2 ± 0.4 nm. As a consistency check of our conversion procedure, we used the measured dielectric constant to calculate the fluence dependence of the p -polarized reflectivity at a 45° angle of incidence. The calculated reflectivity shows excellent agreement with an independent direct measurement of the reflectivity as a function of pump fluence taken at a 45° angle of incidence.

Figure 1 shows the pump-fluence dependence of the real and imaginary parts of the dielectric constant at four different pump-probe time delays. The remarkable feature that stands out in each data set is the combination of a peak in the imaginary part coincident with a zero

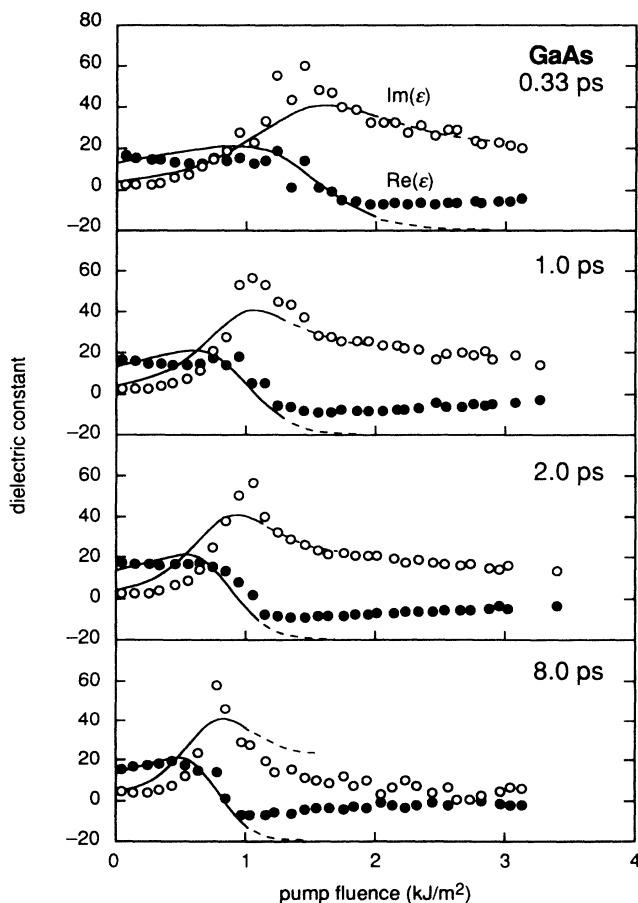


FIG. 1. Dielectric constant at 2.2 eV vs pump fluence for four different pump-probe time delays. The curves through the data are calculated using a single-oscillator model for the dielectric constant. ●, $\text{Re}(\epsilon)$; ○, $\text{Im}(\epsilon)$.

crossing of the real part. The data points in Fig. 2 show the time delays at which the peak and the zero crossing occur for different pump fluences; as the fluence increases, the time delay at which this peak occurs decreases. The minimum fluence at which a peak is observed is 0.8 kJ/m^2 , slightly lower than the threshold of 1.0 kJ/m^2 for permanent damage visible under a microscope. Note finally in Fig. 1 that the peak value of the imaginary part is approximately 60 for all time delays and that at high fluence, beyond the peak, the real and imaginary parts of the dielectric constant exhibit only a slight dependence on the pump fluence.

The peaks in the imaginary part and the coincident zero crossings in the real part of the dielectric constant in Fig. 1 suggest that an absorption peak comes into resonance with the probe frequency. When $\text{Re}(\epsilon) > 0$, the resonant frequency of this absorption peak is above the probe frequency; when $\text{Re}(\epsilon) < 0$, it is below the probe frequency. Figure 1 shows that the resonant frequency starts above the 2.2-eV probe frequency and then sweeps down through it; this effect is seen most clearly for the data points at fluences around 1 kJ/m^2 . The data in Fig. 2 thus show the time at which the resonant frequency reaches the probe frequency for various pump fluences. Evidently, the magnitude and rate of this drop in resonant frequency depend on the strength of the excitation. For fluences below 0.8 kJ/m^2 , the excitation is not strong enough to bring the resonant frequency down to the probe frequency, so the imaginary part of the dielectric constant never reaches the peak value of about 60, and the real part never drops through zero.

The experimental results can be explained by identifying the resonant frequency with the average optical gap of GaAs, which is generally associated with the E_2 absorption peak in the dielectric function.⁵ The data in Fig.

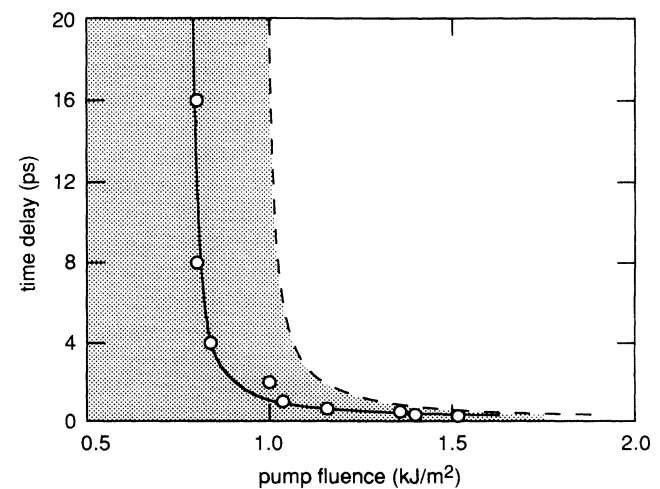


FIG. 2. Pump-probe time delays at which $\text{Im}(\epsilon)$ is maximal and $\text{Re}(\epsilon)=0$ for different pump fluences. The solid line is a fit of Eq. (2) to the data with $\omega_o(\phi, t) = \omega_{\text{probe}}$; the dashed line corresponds to the semiconductor-metal transition where $\omega_o(\phi, t) = \omega_{\text{cr}}$. The single-oscillator model is valid only in the shaded region where GaAs is a semiconductor.

1 then imply that the pump pulse causes the average optical gap to decrease in time. To describe this decrease, we approximate the dielectric function of GaAs using a single-oscillator model with a fluence and time-dependent resonant frequency,

$$\epsilon(\omega) = 1 - \frac{\omega_p^2}{\omega^2 - \omega_o^2(\phi, t) + i\frac{\omega}{\tau}}, \quad (1)$$

where ω_p is the plasma frequency, $\omega_o(\phi, t)$ the resonant frequency of the oscillator, and $1/\tau$ the width of the resonance. In this picture, $\omega_o(\phi, t)$ represents the time- and fluence-dependent average optical gap, with ϕ the pump fluence and t the time delay between the pump and probe pulses.

Fitting Eq. (1) to the dielectric function of unpumped ($\phi=0, t=0$) GaAs,¹⁵ we find $\omega_p = 15.2$ eV, $\omega_o(0,0) = 4.55$ eV, and $\tau = 0.39$ eV⁻¹. The plasma frequency extracted from the fit agrees with the value of 15.5 eV calculated using the total valence electron density of unpumped GaAs.¹⁶ Furthermore, the value obtained for $\omega_o(0,0)$ matches fairly well the 4.75-eV location of the E_2 absorption peak in the dielectric function of unpumped GaAs.^{4,17}

Next, the fluence and time dependence of the resonant frequency ω_o is obtained from the data points in Fig. 2. We describe this dependence empirically using the relation

$$\omega_o(\phi, t) = \omega_o(0,0) - C \left[1 + \frac{T}{t} \right]^{-1} \phi, \quad (2)$$

with C and T constants. Values for C and T are obtained by setting the left-hand side of Eq. (2) equal to the probe frequency, $\omega_o(\phi, t) = 2.2$ eV, and then fitting Eq. (2) to the data points in Fig. 2. Using the value found above for the initial resonant frequency, $\omega_o(0,0) = 4.55$ eV, we find $C = 3.0$ eV kJ⁻¹ m² and $T = 0.34$ ps. Finally, substituting Eq. (2) with the above values for C and T into Eq. (1), we obtain values for the real and imaginary parts of the dielectric constant as a function of fluence and time. The curves in Fig. 1 show these values plotted up to the point where $\omega_o(\phi, t) = 0$.

It should be noted that the single-oscillator model is valid only until the material undergoes a transition to a (semi)metal, i.e., when the conduction-band minimum drops below the valence-band maximum. When this happens ω_o is still greater than zero because ω_o corresponds to the average optical gap, not the band-gap minimum. The single-oscillator model, therefore, is valid only when $\omega_o(\phi, t) > \omega_{cr}$ where ω_{cr} is the value of the average optical gap at the transition. The value of ω_{cr} can be estimated as follows. We assume that the transition takes place for fluences above the observed 1.0-kJ/m² threshold for permanent damage. Then, at the damage threshold, we obtain from Eq. (2) $\omega_{cr} = \omega_o(\phi = 1.0 \text{ kJ/m}^2, t \rightarrow \infty) = 1.6$ eV. Setting the left-hand side of Eq. (2) equal to this critical average optical gap of 1.6 eV, we can now extract the time at which $\omega_o(\phi, t) = \omega_{cr}$ for any pump fluence (see dashed curve in Fig. 2). The validity of the single-oscillator model is therefore limited to the shaded region

in Fig. 2 [$\omega_o(\phi, t) > \omega_{cr}$] and to the corresponding solid portions of the theoretical curves in Fig. 1.

The data in Fig. 1 fully trace the evolution of a laser-induced transformation from semiconductor to metal, with the transition occurring at the points where the solid lines become dashed: (1) Before the transition, the dielectric constant of the semiconductor is well described by a single-oscillator model with a decreasing average optical gap; (2) at the transition, the experimentally measured dielectric constant $\epsilon \approx -10 + 35i$, is independent of time delay, supporting the assumption of a unique value of the critical average optical gap ω_{cr} ; (3) after the transition, the measured dielectric constant is no longer well described by the single-oscillator model. Instead it can be approximated by a Drude model appropriate to a metal. In the Drude model, the carrier density is taken equal to the total valence electron density, and the dc conductivity is a free parameter, which decreases with increasing fluence. The electronic properties in this phase are similar to those seen in liquid carbon produced by femtosecond laser excitation.⁸

The four data series in Fig. 1 can be transformed into one another simply by rescaling the pump-fluence axis. In other words, the evolution of the material response to an excitation of fluence just above 1.0 kJ/m² is essentially the same as that induced by a 2.0-kJ/m² excitation, even though in the former case the transition to a metal takes 8 ps to occur while in the latter case this transition occurs in about 330 fs. This implies that the response of the material to the pump pulse follows essentially a single "path" for all excitation strengths. How far and how fast along this single path the material response progresses depends on the strength of the excitation. The response of the material to the pump pulse can thus be characterized by a single parameter. In the single-oscillator model, this parameter is the average optical gap $\omega_o(\phi, t)$. The fact that the average optical gap is sufficient to describe the data at different time delays indicates that the measured dielectric constant predominantly reflects changes in the electronic band structure. Therefore, other effects such as direct contributions from the optical response of the excited free carriers are relatively small.

What could be the underlying cause of this drastic change in band structure? Major band-structure changes can arise from electronic screening effects or from changes in the lattice structure. Screening by the excited carrier leads to a renormalization of single-particle energies and results in a narrowing of the band gap.¹⁹ If the observed changes in the dielectric constant were due primarily to screening, the average optical gap should be at its minimum immediately after the excitation, when the carrier density is highest, and should then recover as the carrier density relaxes through Auger recombination. This is inconsistent with the decrease in the average optical gap, which only begins with the excitation and at 0.8 kJ/cm², for instance, continues for picoseconds.

A change in the lattice structure, on the other hand, evolves on a time scale longer than the duration of the excitation. Structural transformations induced under high pressure²⁰ and under thermal melting^{21,22} have been observed to lead to a collapse of the band gap. In general,

lattice destabilization in covalent solids leads to a structure with a higher coordination number and metallic characteristics; calculations have shown that a 10% change in bond length is sufficient for the semiconductor to become a metal.²⁰ For such displacements to be achieved on a picosecond time scale, the ions would need to move at a speed of only 25 m/s. Changes in lattice structure, therefore, could produce changes in the band structure which are consistent with the observed changes in the dielectric constant.

In our experiment, the change in the lattice structure is driven directly by the optical excitation of electrons. If the femtosecond laser pulse excites enough electrons from bonding valence states to antibonding conduction states, the lattice becomes unstable. As the lattice dis-

torts, the average bonding-antibonding splitting decreases, which is manifested optically by a decrease in the average optical gap. A transition from semiconductor to (semi)metal occurs when the average bonding-antibonding splitting decreases so far that the conduction-band minimum drops below the valence-band maximum.

The authors thank Professor N. Bloembergen, Professor H. Ehrenreich, and Professor E. Kaxiras for many insightful comments. E.G. gratefully acknowledges support from the Fannie and John Hertz Foundation. This work was supported by Contracts Nos. ONR N00014-89-J-1023 and NSF DMR 89-20490.

-
- ¹J. A. Van Vechten, R. Tsu, and F. W. Saris, *Phys. Lett.* **74A**, 422 (1979).
- ²R. Biswas and V. Ambegoakar, *Phys. Rev. B* **26**, 1980 (1982).
- ³P. Stampfli and K. H. Bennemann, *Phys. Rev. B* **42**, 7163 (1990).
- ⁴W. A. Harrison, *Electronic Structure and the Properties of Solids: The Physics of the Chemical Bond* (Dover, New York, 1989).
- ⁵M. L. Cohen and J. R. Chelikowsky, *Electronic Structure and Optical Properties of Semiconductors* (Springer-Verlag, Berlin, 1988).
- ⁶R. W. Schönlein, W. Z. Lin, J. G. Fujimoto, and G. L. Eesley, *Phys. Rev. Lett.* **58**, 1680 (1987).
- ⁷J. A. Kash, J. C. Tsang, and J. M. Hvam, *Phys. Rev. Lett.* **54**, 2151 (1985).
- ⁸E. J. Yoffa, *Phys. Rev. B* **21**, 2415 (1980).
- ⁹H. W. K. Tom, G. D. Aumiller, and C. H. Brito-Cruz, *Phys. Rev. Lett.* **60**, 1438 (1988).
- ¹⁰P. N. Saeta, J.-K. Wang, Y. Siegal, N. Bloembergen, and E. Mazur, *Phys. Rev. Lett.* **67**, 1023 (1991).
- ¹¹T. Schröder, W. Rudolph, S. V. Govorkov, and I. L. Shumai, *Appl. Phys. A* **51**, 1438 (1990).
- ¹²D. L. Greenaway and G. Harbeke, *Optical Properties and Band Structure of Semiconductors* (Pergamon, London, 1968).
- ¹³J.-K. Wang, Y. Siegal, C. Z. Lü, and E. Mazur, *Opt. Commun.* **91**, 77 (1992).
- ¹⁴R. F. Potter, in *Optical Properties of Solids*, edited by S. Nudelman and S. S. Mitra (Plenum, New York, 1969).
- ¹⁵E. D. Palik, in *Handbook of Optical Constants of Solids*, edited by E. D. Palik (Academic, New York, 1985), p. 434.
- ¹⁶H. R. Philipp and H. Ehrenreich, *Phys. Rev.* **129**, 1550 (1963).
- ¹⁷D. E. Aspnes, G. P. Schwartz, G. J. Gualtieri, A. A. Studna, and B. Schwartz, *J. Electrochem. Soc.* **128**, 590 (1981).
- ¹⁸D. H. Reitze, H. Ahn, and M. C. Downer, *Phys. Rev. B* **45**, 2677 (1992).
- ¹⁹H. Kalt and M. Rinker, *Phys. Rev. B* **45**, 1139 (1992).
- ²⁰S. Froyen and M. L. Cohen, *Phys. Rev. B* **28**, 3258 (1983).
- ²¹V. M. Glazov, S. N. Chizhevskaya, and N. N. Glagoleva, *Liquid Semiconductors* (Plenum, New York, 1969).
- ²²W. Jank and J. Hafner, *J. Non-Cryst. Solids* **114**, 16 (1989).

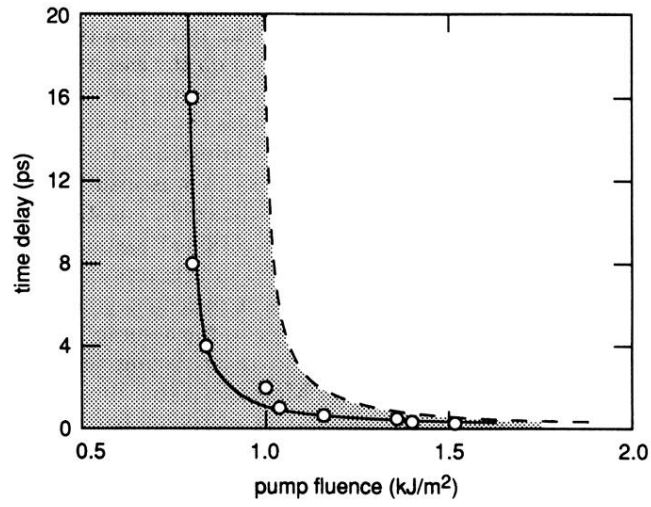


FIG. 2. Pump-probe time delays at which $\text{Im}(\epsilon)$ is maximal and $\text{Re}(\epsilon)=0$ for different pump fluences. The solid line is a fit of Eq. (2) to the data with $\omega_o(\phi, t)=\omega_{\text{probe}}$; the dashed line corresponds to the semiconductor-metal transition where $\omega_o(\phi, t)=\omega_{\text{cr}}$. The single-oscillator model is valid only in the shaded region where GaAs is a semiconductor.